Acta Cryst. (1996). A52, 47–55

X-ray Standing Waves in Crystals Distorted by a Constant Strain Gradient. A Theoretical Study

F. N. CHUKHOVSKII,† C. MALGRANGE* AND J. GRONKOWSKI‡

Laboratoire de Minéralogie-Cristallographie, associé au CNRS, Universités Pierre et Marie Curie (Paris VI) et Denis Diderot (Paris VII), Tour 16, case 115, 4, place Jussieu, 75252 Paris, France. E-mail: malgrange@lmcp.jussieu.fr

(*Received 31 March 1995; accepted 3 July 1995*)

Abstract

X-ray Bragg-case diffraction in crystals distorted by a constant strain gradient is studied theoretically. The rocking curves and intensity distributions of the standing-wave fields are calculated for several data sets corresponding to real physical cases of diffraction in bent crystals (Si 111 reflection and Mo $K\alpha_1$ radiation, GaAs 004 reflection and Cu $K\alpha_1$ radiation, PbTe 002 reflection and Cr $K\alpha_1$ radiation). The obtained curves are interpreted using the quasi-classical approximation of the exact analytical solution of the problem. The oscillations on one flank of the rocking curves are shown to result from interference between the wave directly reflected at the crystal surface and the one issued from the wave field deflected back to the surface along a curved trajectory. Formulae for their distances are also derived. The sensitivity of the rocking curves and X-ray standing waves to the crystal curvature and absorption is discussed. In particular, the phase shift between the oscillations in the rocking curve and in the standing-wave intensity profile can be readily used to determine the positions of atoms in the bent crystal or at its surface.

1 Introduction

The X-ray standing-wave technique (XSW) is now a well established tool to determine with a high accuracy the position of foreign atoms (*e.g.* adsorbed on the crystal surface or diffused into the crystal) with respect to the crystalline lattice. It is particularly well adapted (and consequently most often employed) to studies of surfaces and interfaces.

The principle of the technique, proposed by Batterman (1964, 1969), which was realized experimentally for the first time by Kjaer Andersen, Golovchenko & Mair (1976) and has been developed since then in many papers [see Malgrange & Ferret (1992) and Zegenhagen (1993) for recent reviews and further references], is based on the coupling between the diffracted and forward-diffracted waves in a crystal undergoing dynamical diffraction. Interference between these two waves gives rise to a standing wave field inside and above the crystal. Its electric displacement $\mathbf{D}$ at a point $\mathbf{r}$ is given by

$$\mathbf{D} = \mathbf{D}_o \exp(i\mathbf{K}_o \cdot \mathbf{r}) + \mathbf{D}_h \exp(i\mathbf{K}_h \cdot \mathbf{r}), \quad (1)$$

where $\mathbf{D}_o$ and $\mathbf{D}_h$ are the pseudoamplitudes (complex, vector and constant) of the waves in the forward-diffracted and diffracted directions, respectively, $\mathbf{K}_o$ and $\mathbf{K}_h = \mathbf{K}_o + \mathbf{h}$ are their wave vectors, $\mathbf{h}$ is the reciprocal-lattice vector.

If, for simplicity, an incident plane wave polarized perpendicularly to the plane of diffraction is assumed, one can write

$$|\mathbf{D}|^2 = |D_o|^2[1 + |\xi_p|^2 + 2|\xi_p| \cos(\mathbf{h} \cdot \mathbf{r} + \psi_p)], \quad (2)$$

where D_o and D_h are the pseudoamplitudes (complex, scalar and constant) of the forward-diffracted and diffracted waves, respectively, and

$$\xi_p = D_h/D_o = |\xi_p| \exp(i\psi_p). \quad (3)$$

In a perfect crystal, $\mathbf{h} \cdot \mathbf{r} = 2\pi(N + \Delta d/d)$, where N is an integer, d is the spacing of the diffracting planes and Δd is the distance from a point located at $\mathbf{r}$ to the nearest diffracting plane. The modulus and the phase ψ_p of ξ_p are functions of the departure of the incident wave $\Delta\vartheta$ from the Bragg angle. Since ψ_p varies by π when passing from the low-angle side of the diffraction profile to the high-angle one, curves representing $|\mathbf{D}|^2$ as a function of $\Delta\vartheta$ depend strongly on the value of $\Delta d/d$. By measuring at the same time the rocking curve and a signal proportional to $|\mathbf{D}|^2$ (for instance, the intensity of fluorescence of adsorbed atoms or the flux of photoelectrons), one can determine with a high accuracy the $\Delta d/d$ values for these atoms, *i.e.* their position with respect to the bulk lattice.

XSW's are now widely used for various applications. However, while the basic dynamical theory for perfect crystals is well known and established, XSW's in distorted crystals have only rarely been discussed; numerical solutions of the Takagi–Taupin equations (Takagi 1962, 1969; Taupin 1964) were obtained for a crystal

† Permanent address: Institute of Crystallography, Russian Academy of Sciences, Leninsky prospekt 59, 117333 Moscow, Russia.

‡ Permanent address: Institute of Experimental Physics, University of Warsaw, Poland.

with a transition layer (Authier, Gronkowski & Malgrange, 1989) and a crystal with a linear gradient of the parameter normal to the crystal surface (Vartanyantz, Kovalchuk & Beresovsky, 1993). The aim of the present paper is a detailed theoretical study of the rocking curve and the standing-wave field for crystals distorted by a uniform strain gradient.

2. Exact analytical solution for the crystal with a constant strain gradient

The electric displacement in a distorted crystal is a function of the position vector **r**:

$$\mathbf{D}(\mathbf{r}) = \mathbf{D}_o(\mathbf{r}) \exp(i\mathbf{K}_o \cdot \mathbf{r}) + \mathbf{D}_h(\mathbf{r}) \exp(i\mathbf{K}_h \cdot \mathbf{r}), \quad (4)$$

where $\mathbf{K}_h = \mathbf{K}_o + \mathbf{h}$, **h** being the (constant) reciprocal-lattice vector for the perfect crystal. Consequently, the normalized squared electric displacement defined as $Y(\mathbf{r}) = |\mathbf{D}(\mathbf{r})|^2/|D_o(\mathbf{r})|^2$ is

$$Y(\mathbf{r}) = 1 + |\xi(\mathbf{r})|^2 + 2|\xi(\mathbf{r})| \cos[\mathbf{h} \cdot \mathbf{r} + \psi(\mathbf{r})], \quad (5)$$

where $\psi(\mathbf{r})$ is the phase of $\xi(\mathbf{r}) = D_h/D_o$ [*cf.* (3)].

Chukhovskii, Gabrielyan & Petrashen' (1978) have given formulae that allow one to obtain the pseudo-amplitudes D_o and D_h at every point of the crystal by integrating the corresponding Green functions, multiplied by the amplitude of the incident wave, along the entrance surface of the crystal. They analysed the special case where the phase of the incident wave along the entrance surface varies linearly with the coordinates, *i.e.* for a plane wave incident on a flat crystal with a distortion such that

$$\mathbf{h} \cdot \mathbf{u}(\mathbf{r}) = -2BZ^2, \quad (6)$$

where Z is a reduced coordinate along the normal to the surface: $Z = z\pi/\Lambda$, z being the usual coordinate and Λ the extinction length. For such a case, they performed the integration and obtained the following formula for D_h/D_o:

$$\xi = -i(\chi_h/\chi_{\bar{h}})(1 + i\kappa)\tilde{\nu}^{1/2} \times [D_{-1-\nu}(y)/D_{-\nu}(y)] \exp(2iBZ^2), \quad (7)$$

where $D_{-n-\nu}$ is the parabolic cylinder function of order $(-n - \nu)$; $\kappa = \mathcal{J}(\chi_h\chi_{\bar{h}})^{1/2}/\mathcal{R}(\chi_h\chi_{\bar{h}})^{1/2}$ [$\kappa < 0$ due to the form of the waves chosen in (1)]; χ_h and $\chi_{\bar{h}}$ are the h and $\bar{h}$ Fourier coefficients of the dielectric susceptibility; $\mathcal{R}$ means the real part of a complex number, $\mathcal{J}$ is its imaginary part; $y = -2\eta\tilde{\nu}^{1/2}$; $\tilde{\nu} = i/4B$; $\nu = \tilde{\nu}(1 + i\kappa)^2$; the constant strain gradient $4B$ is defined as $4B = \partial^2(\mathbf{h} \cdot \mathbf{u})/\partial S_o \partial S_h$, where S_o and S_h are reduced (dimensionless) coordinates related to the usual oblique coordinates s_o and s_h by $S_o = s_o\pi \sin\vartheta_B/\Lambda$ and $S_h = s_h\pi \sin\vartheta_B/\Lambda$, respectively; the (dimensionless) incidence parameter η_o proportional to $\Delta\vartheta$ is given by

$$\eta_o = (\Delta\vartheta \sin 2\vartheta_B + \chi_o)/\mathcal{R}(\chi_h\chi_{\bar{h}})^{1/2}; \quad (8)$$

$\Delta\vartheta = \vartheta - \vartheta_B$ is the departure of the incidence angle ϑ from the Bragg angle ϑ_B; η is the local value of the incidence parameter, which varies during the propagation of wave fields in the crystal according to the relation

$$\eta = \eta_0 + 4BZ. \quad (9)$$

The strain parameter $4B$ is related to the β parameter defined by Kato (1964) by the simple relation $4B = \beta/\beta_c$, where $\beta_c = \pi/(2\Lambda_o)$ is the critical value of the strain gradient introduced by Authier & Balibar (1970); $\Lambda_o = \Lambda/\tan\vartheta_B$ represents the inverse of the distance between the apices of the dispersion surface and is characteristic of the crystal and the reflection.

The imaginary part of the incidence parameter, $\eta_i = \mathcal{J}(\chi_o)/\mathcal{R}(\chi_h\chi_{\bar{h}})^{1/2}$, is directly related to the normal linear absorption coefficient μ_0 through the formula $\eta_i = \lambda\mu_0/[4\pi\mathcal{R}(\chi_h\chi_{\bar{h}})^{1/2}]$. Notice that here $\mathcal{J}(\chi_o)$ and η_i are positive due to the choice of the form of the exponentials describing the waves in (1).

All these expressions apply to the symmetric Bragg case and σ polarization; for the π polarization, both χ_h and $\chi_{\bar{h}}$ have to be multiplied by $\cos 2\vartheta_B$.

It can be shown that the condition of linearity of the phase along the entrance surface, necessary to obtain (7), is also satisfied in the case of a cylindrically bent crystal if the incident wave is spherical and issued from a point that lies on the Rowland circle. The displacement field $\mathbf{u} = [u_x, u_y, u_z]$ can then be written as

$$\begin{aligned} u_x &= xz/R + (s_{51}/s_{11})z^2/2R \\ u_y &= 0 \\ u_z &= -x^2/R + (s_{31}/s_{11})z^2/2R, \end{aligned} \quad (10)$$

where R is the radius of curvature and s_{ij} are the components of the compliance tensor characterizing the anisotropic properties of the elastically bent crystal. The product $\mathbf{h} \cdot \mathbf{u}(\mathbf{r})$ is a quadratic function of S_o and S_h and can be written as $\mathbf{h} \cdot \mathbf{u}(\mathbf{r}) = 2(AS_o^2 + 2BS_oS_h + CS_h^2)$. Integration of the Green function along the entrance surface gives

$$\xi = -i(\chi_h/\chi_{\bar{h}})(1 + i\kappa)\tilde{\nu}^{1/2}[D_{-1-\nu}(y)/D_{-\nu}(y)] \times \exp[-i\mathbf{h} \cdot \mathbf{u}(\mathbf{r})], \quad (11)$$

which is equivalent to (7) but valid for the cylindrically bent crystal as well; ξ is again a function of y, which also for this more general case is a function of B [see the formula for y, given after (7), and (9) for η which is still valid].

It is readily seen that the coefficients A and C characterizing the constant strain gradient appear in (11) only in the phase factor $\exp[-i\mathbf{h}\cdot\mathbf{u}(\mathbf{r})]$; the important term is the one with the mixed derivative, as $4B$ appears in y and in $\tilde{\nu}$.

In the further course of this work, the analytical results will be illustrated with numerical results obtained for several physical cases. The numerical calculations are made for the case of a depth-dependent deformation [given by (6)] because then, instead of the full Takagi–Taupin theory with its set of partial differential equations, the one-dimensional version due to Taupin (1964) with a single ordinary differential equation (the 'Taupin equation') can be used. However, it is to be stressed that the whole discussion applies also in the case of a cylindrically bent anisotropic crystal and the source of X-rays on the Rowland circle.

3. Propagation of X-ray wave fields in distorted crystals

Some useful results, concerning the propagation of X-ray beams inside crystals distorted by a constant strain gradient and obtained first by Gronkowski & Malgrange (1984) through computer simulations and then analytically by Chukhovskii & Malgrange (1989), will be briefly recalled here. X-ray waves incident on such crystals with a departure from the Bragg angle $\Delta\vartheta$ outside the domain of quasi-total reflection (called hereafter, to simplify, the domain of 'total' reflection) propagate inside the crystal along hyperbolic paths. The sign of their curvature depends on the value of η_o. For $\eta_r = \mathcal{R}(\eta_o)$ on one side of the rocking curve, the beam paths are curved towards the surface of the crystal; this side corresponds to $\eta_r < -1$ if $B > 0$ and $\eta_r > 1$ if $B < 0$ (Fig. 1). On the other side (corresponding to $\eta_r > 1$ if $B > 0$ and $\eta_r < -1$ if $B < 0$), they are curved towards the inside of the crystal.

These properties of beam paths in the crystal allow one to interpret physically some results first obtained by Taupin (1964) [recently also by Vartanyantz, Kovalchuk & Beresovsky (1993), Uschmann, Förster, Gäbel, Hölzer & Ensslen (1993) and Krisch (1993)]. The rocking curves for crystals with a constant strain gradient present oscillations of intensity on one side

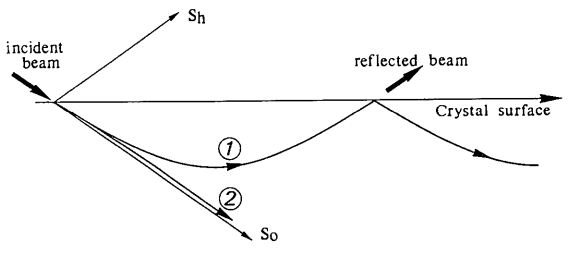

Fig. 1. Ray trajectories in a crystal with a constant strain gradient in the symmetric Bragg case, $B > 0$: (1) $\eta_r < -1$; (2) $\eta_r > 1$.

Table 1. *Values of physical parameters for the studied cases*

μ_0 is the linear absorption coefficient, $\eta_i = \mathcal{J}(\eta_0)$ is the imaginary part of the incidence parameter, $\kappa = \mathcal{J}(\chi_h\chi_{\bar{h}})^{1/2}/\mathcal{R}(\chi_h\chi_{\bar{h}})^{1/2}$, R is the radius of curvature of a bent crystal, corresponding to the given physical case (rows) and the value of strain gradient (columns *a*–*c*).

Physical case	μ_0 (cm^{-1})	η_i	κ	R (m) *a*	*b*	*c*
Si(111), Mo $K\alpha_1$	14	0.0095	−0.0066	127	24	4.5
GaAs(004), Cu $K\alpha_1$	343	0.0503	−0.0467	9.44	1.8	0.34
PbTe(002), Cr $K\alpha_1$	5548	0.2667	−0.2544	0.56	0.11	0.02

which, as will be shown in the further course of this work, are due to interference between the wave directly reflected at the crystal surface and the wave issued from a wave field propagating along a path curved back to the surface. This phenomenon occurs only on one flank of the rocking curve, which will be called here the 'oscillating wing' (as opposed to the 'ordinary wing').

4. Numerical solutions for a crystal with a constant strain gradient

In order to visualize the full character of the results obtained for the case of constant strain gradient, a numerical program for solving the Taupin equation, described elsewhere (Gronkowski, 1991), was used. The results of the calculations of the rocking curves and the normalized squared induction at the crystal surface are presented in Figs. 2 and 3, respectively.

The calculations were made for three values of the strain gradient $4B$: 0.0285, 0.15 and 0.8 [shown in Figs. 2 and 3 in columns (*a*), (*b*) and (*c*), respectively]. Three physical cases of symmetric Bragg diffraction with various radiations on different crystals were chosen to include in the study also the role of absorption. The lower row corresponds to 111 reflection from silicon, taken with Mo $K\alpha_1$ radiation (weak absorption), the middle row to 004 reflection from GaAs, taken with Cu $K\alpha_1$ radiation (strong absorption), and the upper row to 002 reflection from PbTe, taken with Cr $K\alpha_1$ radiation (extremely strong absorption). The values of various parameters for these three cases are given in Table 1.

One readily sees the most characteristic feature of the rocking curves – their oscillating wing. As $B > 0$, it is always the left one (with $\eta_r < -1$). The period of oscillations increases with B and their attenuation depends strongly both on the absorption and the value of B (see next section for a discussion).

For weak deformations, the rocking curves in the domain of 'total' reflection and on the ordinary wing are almost identical to those for perfect crystals [Fig. 2(*a*)]. The oscillations on the oscillating wing are very densely spaced and obviously it would not be possible to obtain evidence of them in a real experiment.

The Y curves (corresponding to the XSW signal for $\mathbf{h}\cdot\mathbf{r} = 0$) also exhibit fringes with the same distances as those in the respective rocking curves which – especially for strong gradients and weak absorption [Fig. 3(*c*)(i)] – change the XSW signal dramatically. However, even for extremely strong absorption [Fig. 3(iii)], the XSW signal differs from the perfect-crystal one not only through the oscillations but also in the relation of the intensities on the left and right flanks of the 'total' reflection domain.

5. Discussion of the analytical solution

5.1. *Quasi-classical approximation of the analytical solution*

We shall use, as in an earlier paper (Chukhovskii & Malgrange, 1989), the quasi-classical approximation of the parabolic cylinder functions $D_{-n-\nu}(y)$, which is valid for $|y^2 + 4\nu|^{1/2} \gg 1$. In this approximation, the $D_{-n-\nu}$ functions are written as a sum of two exponential functions given in Appendix *A*, where it is also shown that the second term vanishes for incidence parameters corresponding to the ordinary wing and is negligible in the domain of 'total' reflection. In these cases, the ratio of the parabolic cylinder functions may be written as (see Appendix *A*)

$$D_{-1-\nu}(y)/D_{-\nu}(y) = \tilde{\nu}^{-1/2} i/\{\eta + [\eta^2 - (1+i\kappa)^2]^{1/2}\}. \quad (12)$$

Substituting (12) into (11), one gets

$$\xi = (\chi_h/\chi_{\bar{h}})\big((1+i\kappa)/\{\eta + [\eta^2 - (1+i\kappa)^2]^{1/2}\}\big) \times \exp[-i\mathbf{h}\cdot\mathbf{u}(\mathbf{r})], \quad (13)$$

which, apart from the factor $\exp[-i\mathbf{h}\cdot\mathbf{u}(\mathbf{r})]$, is exactly the value of ξ_p for a perfect infinitely thick crystal receiving an incident plane wave characterized by the incidence parameter η.

Let us then write

$$\xi = |\xi_p(\eta)| \exp[i\psi_p(\eta)] \exp[-i\mathbf{h}\cdot\mathbf{u}(\mathbf{r})], \quad (14)$$

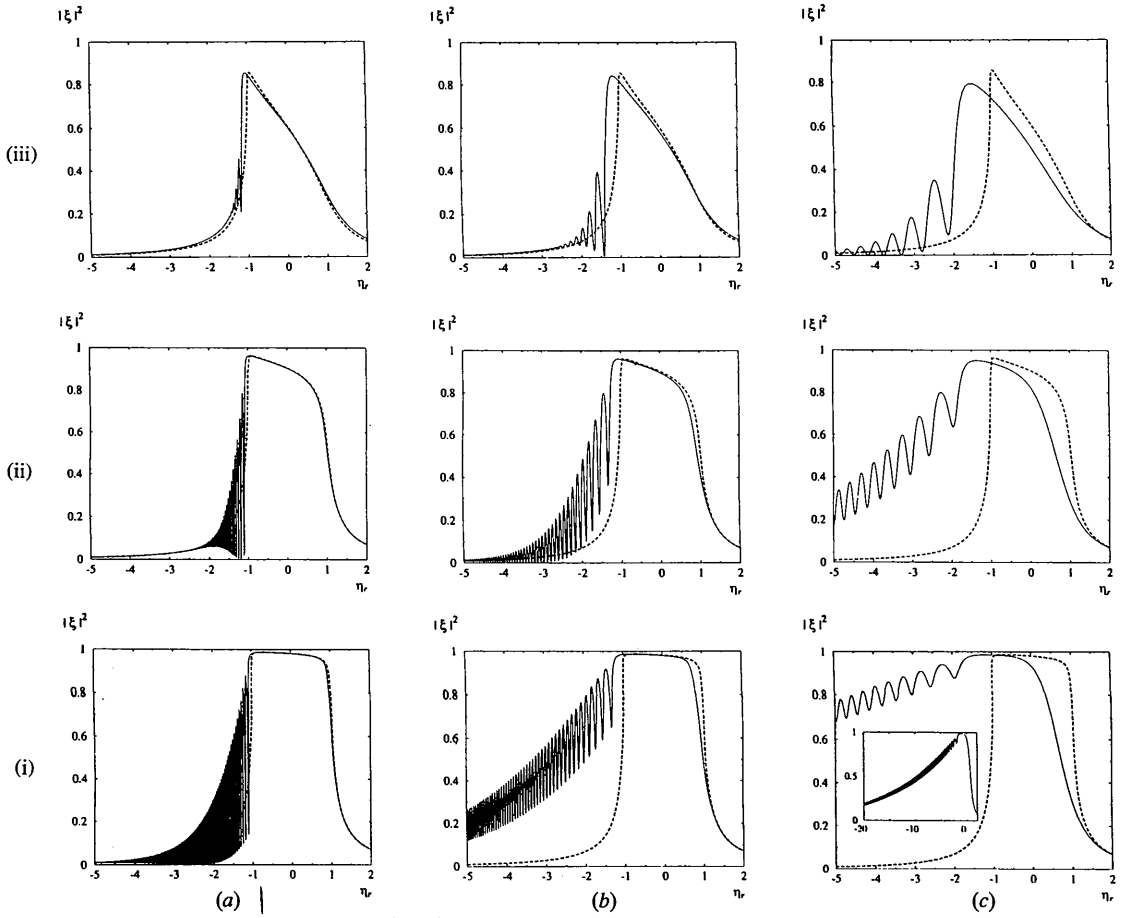

Fig. 2. Rocking curves for crystals with a constant strain gradient: (*a*) $4B = 0.0285$, (*b*) $4B = 0.15$, (*c*) $4B = 0.8$. (i) 111 reflection from silicon, taken with Mo $K\alpha_1$ radiation [the inset in (*c*)(i) shows the rocking curve in a larger range of $-20 \le \eta_r \le 2$]; (ii) 004 reflection from GaAs, taken with Cu $K\alpha_1$ radiation; (iii) 002 reflection from PbTe, taken with Cr $K\alpha_1$ radiation. The dashed lines represent the rocking curves for the perfect crystals.

where $|\xi_p(\eta)|$ and $\psi_p(\eta)$ are the modulus and the phase of ξ_p. Then, from (5), the total electric induction in the distorted crystal is expressed as

$$\begin{aligned}|\mathbf{D}|^2 &= |D_o|^2\big(1+|\xi_p(\eta)|^2+2|\xi_p(\eta)| \\ &\quad\times\cos\{\mathbf{h}\cdot\mathbf{r}+\psi_p(\eta)-\mathbf{h}\cdot\mathbf{u}(\mathbf{r})\}\big) \\ &= |D_o|^2\big(1+|\xi_p(\eta)|^2+2|\xi_p(\eta)| \\ &\quad\times\cos\{\mathbf{h}\cdot[\mathbf{r}-\mathbf{u}(\mathbf{r})]+\psi_p(\eta)\}\big), \qquad (15)\end{aligned}$$

$\mathbf{r}$ being the position vector in the distorted crystal. Let us call $\mathbf{r}_p$ the position vector of the same point before the deformation was introduced:

$$\mathbf{h}\cdot[\mathbf{r}-\mathbf{u}(\mathbf{r})]=\mathbf{h}\cdot\mathbf{r}_p=2\pi(N+\Delta d/d), \qquad (16)$$

where N is an integer, equal to the number of diffracting planes between the origin and the considered point whose distance to the nearest diffracting plane is Δd. Therefore,

$$Y=1+|\xi_p(\eta)|^2+2|\xi_p(\eta)|\cos[2\pi\Delta d/d+\psi_p(\eta)]. \qquad (17)$$

From (17), it can be concluded that (under the condition of validity of the quasi-classical approximation) for local η values inside the domain of 'total' reflection and on the ordinary wing of the rocking curve the XSW intensity can be considered as corresponding to the 'tangent' perfect crystal, *i.e.* the one that would receive a wave with the incidence parameter equal to the local parameter η [obtained from (9) for given η_o and $4B$].

The domain of validity of the quasi-classical approximation is defined by a condition on the modulus of $(y^2+4\nu)^{1/2}$ (see Appendix *A*):

$$\begin{aligned}|y^2+4\nu|^{1/2} &= |B|^{-1/2}[(1-\eta_r^2+\eta_i^2-\kappa^2)^2 \\ &\quad+4(\kappa-\eta_r\eta_i)^2]^{1/4} \\ &\gg 1. \qquad (18)\end{aligned}$$

Since $\eta_i > |\kappa|$, condition (18) may be replaced for the sake of discussion by a more stringent (and simpler) one:

$$|1-\eta_r^2|^{1/2}/|B|^{1/2}\gg 1. \qquad (19)$$

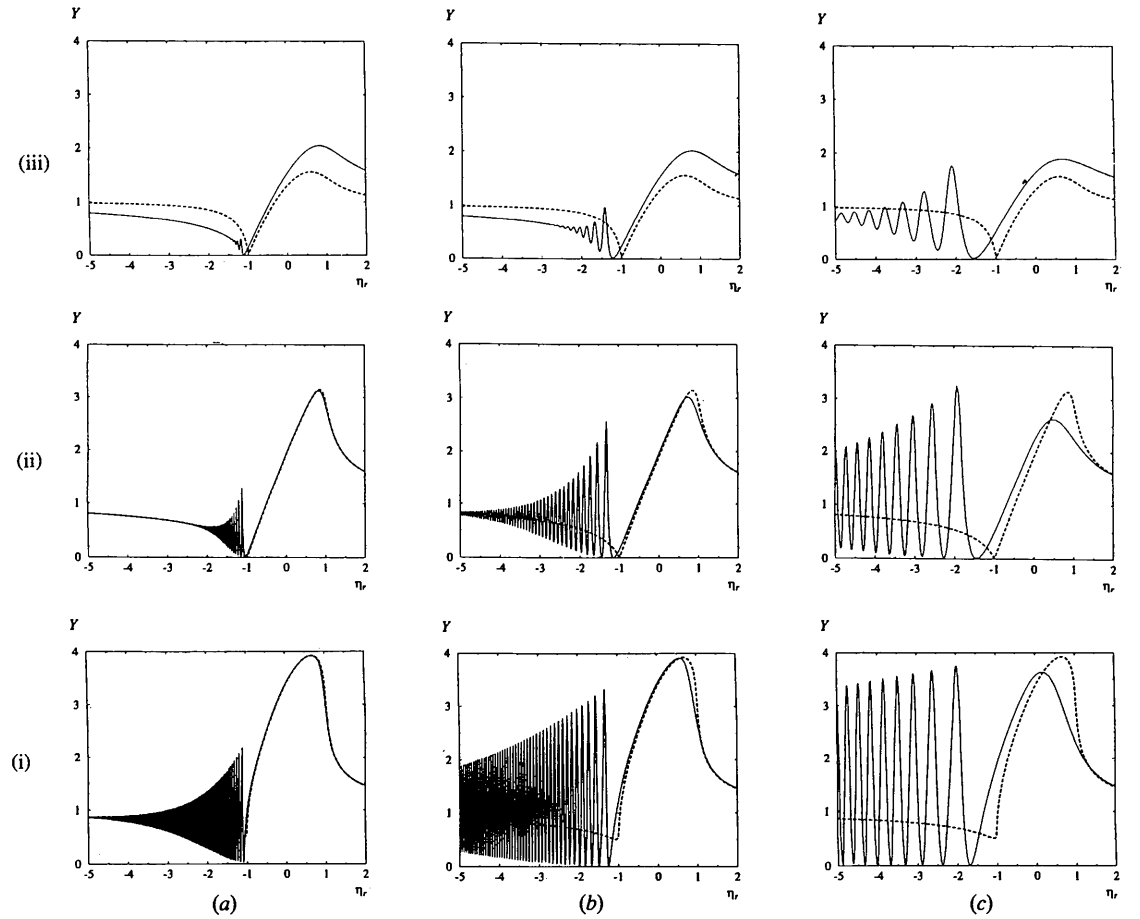

Fig. 3. The normalized wave-field intensity Y in crystals with a constant strain gradient, calculated for $\mathbf{h}\cdot\mathbf{r}=0$, as a function of the dimensionless deviation parameter η_r [see caption to Fig. 2 for explanations of (*a*)–(*c*) and (i)–(iii)].

Table 2. *The domain of validity of the quasi-classical approximation for various values of 4B*

$\lvert 4B\rvert = 0.001$	$\lvert 4B\rvert = 0.0285$	$\lvert 4B\rvert = 0.15$	$\lvert 4B\rvert = 0.8$
$\lvert\eta_r\rvert < 0.987$, $\lvert\eta_r\rvert > 1.012$	$\lvert\eta_r\rvert < 0.54$, $\lvert\eta_r\rvert > 1.31$	$\lvert\eta_r\rvert > 2.8$	$\lvert\eta_r\rvert > 4.6$

If we assume that condition (19) is satisfied if its left-hand side is greater than 10:

$$|1 - \eta_r^2|^{1/2}/|B|^{1/2} > 10, \tag{20}$$

then, after simple manipulations with inequality (20), its domain of validity can easily be obtained. The results of such a procedure for four different values of B are summarized in Table 2. It is seen that, for the smallest values of the strain gradient ($|B|$ of the order of 0.001), condition (20) is fulfilled everywhere except in a small domain around $|\eta_r| = 1$. For larger values of $|B|$, condition (20) is not satisfied in a larger domain.

5.2. *The physical origin of the oscillations and the role of absorption*

It is clear that the second term in the development of the parabolic cylinder functions $D_{n-\nu}$ (see Appendix A) represents the diffracted wave in the wave field deflected towards the crystal surface while the first term corresponds to the wave diffracted directly at the surface. It is interesting to discuss the ratio of these two terms [in (25), see Appendix A], equal to $\exp(2\theta_{n+\nu})\exp[i\pi(n+\nu)]$. It can be shown that the modulus of this ratio is an exponentially decreasing function if $\eta_i > 4B/3$ independently of the value of η_r. On the other hand, for $\eta_i < 4B/3$, the second term is greater than the first one. The smaller η_i is with respect to $4B/3$, the more the second term becomes larger, which results both in an increase of the half-width of the rocking curve and a decrease in the contrast of the oscillations, because then the interferences take place between two terms of very different values.

When η_i does not differ very much from $4B/3$, the two terms are of the same order and, consequently, the amplitude of the oscillations attains the greatest values; however, the averaged shape of the rocking curve is hardly different from the perfect one.

When $\eta_i > 4B/3$, the amplitude of the curved wave field is smaller than the amplitude of the wave diffracted directly at the surface. Consequently, the rocking curve is not widened and the amplitude of the oscillations is small, becoming practically zero for $\eta_i \gg 4B/3$.

These analytical results can be checked on the calculated rocking curves (Fig. 2) where the values of $4B$ were chosen in such a way that, for the cases on the diagonal [Figs. 2(*a*)(i), (*b*)(ii) and (*c*)(iii)], the condition $\eta_i = 4B/3$ is satisfied. When $4B/3 > \eta_i$, the half-width of the rocking curve indeed gets larger than the Darwin width [Figs. 2(*b*)(i), (*c*)(i), (*c*)(ii)] and the oscillations are strong and easily visible. On the other hand, when $4B/3 < \eta_i$, the half-width practically does not change [Figs. 2(*a*)(ii), (*a*)(iii), (*b*)(iii)]. Nevertheless, oscillations are still present, since there is still some intensity left in the wave fields deflected to the surface, especially the ones with smaller $|\eta_r|$ that have not traversed a long path in the crystal.

5.3. *The oscillations near the limit of the 'total' reflection domain*

In order to explore the flanks of the rocking curves close to the limit of the 'total' reflection region, it is necessary to go back to the differential equations that define the $D_{-n-\nu}$ functions. In the domain of $|\eta_r| \simeq 1$, the term $\eta_r^2 - 1$ can be approximated as $2(\eta_r - 1)$ if $\eta_r \simeq 1$ or $-2(\eta_r + 1)$ if $\eta_r \simeq -1$. The two cases have to be distinguished, but in both of them the basic differential equation can be written as

$$\partial^2 f/\partial\zeta^2 - \zeta f = 0. \tag{21}$$

Its solution is the Airy function $\mathrm{Ai}(\zeta)$; ζ is a new variable, which is not exactly the same for the two signs of η_r.

Depending on the sign of $\mathcal{R}(\zeta)$, the Airy function $\mathrm{Ai}(\zeta)$ is tabulated or has to be transformed in a sum of two functions that are tabulated. In order to illustrate the results, let us assume $B > 0$. Then, on the side of the rocking curve where $\eta_r < -1$ (but not very different from $\eta_r = -1$), the Airy function is written as

$$\mathrm{Ai}(\zeta) = [(-\zeta)^{1/2}/3]\{J_{-1/3}[\tfrac{2}{3}(-\zeta)^{3/2}] + J_{1/3}[\tfrac{2}{3}(-\zeta)^{3/2}]\}, \tag{22}$$

where $J_{-1/3}$ and $J_{1/3}$ are the ordinary Bessel functions. They have an oscillatory character and their asymptotic developments are cosine functions. If, for the sake of simplicity, absorption is neglected, then these developments give for the Airy function $\cos\{2[-2(\eta_r + 1)]^{2/3}|\tilde{\nu}|/3 - \pi/4\}$. Thus, it is possible to deduce the period of the oscillations of the rocking curve near $\eta_r = -1$:

$$T_1 = 2\pi B/[2(-\eta_r - 1)]^{1/2}. \tag{23}$$

Table 3 shows the values calculated with formula (23) as compared with the values obtained from the full numerical calculations. It is readily seen that the approximate formula (23) works really well only for the values of $|\eta_r|$ very close to 1 (*i.e.* for small values of the strain gradient that lead to very condensed fringes).

5.4. *The oscillations far from the 'total' reflection domain*

If it is assumed that the oscillations of the intensity are caused by the interference between the wave fields

Table 3. *Comparison of the values of $T_1^{(c)}$ obtained through full calculations for Si(111), Mo $K\alpha_1$ and $T_1^{(t)}$ obtained from formula (23)*

$4B = 0.001$			$4B = 0.0285$			$4B = 0.15$		
η_r	$T_1^{(c)}$	$T_1^{(t)}$	η_r	$T_1^{(c)}$	$T_1^{(t)}$	η_r	$T_1^{(c)}$	$T_1^{(t)}$
−1.0200	0.0079	0.0079	−1.184	0.074	0.074	−1.541	0.206	0.228
−1.0272	0.0067	0.0067	−1.250	0.059	0.063	−1.729	0.170	0.196
−1.0336	0.0061	0.0061	−1.306	0.053	0.057	−1.886	0.145	0.178
−1.0395	0.0056	0.0056	−1.357	0.048	0.053	−2.026	0.134	0.165
−1.0450	0.0052	0.0052	−1.404	0.046	0.050	–	–	–

Table 4. *Comparison of the values of $T_2^{(c)}$ obtained through full calculations [from the curves in Fig. 2(i)] and $T_2^{(t)}$ obtained from formula (24)*

$4B = 0.0285$			$4B = 0.15$			$4B = 0.8$		
η_r	$T_2^{(c)}$	$T_2^{(t)}$	η_r	$T_2^{(c)}$	$T_2^{(t)}$	η_r	$T_2^{(c)}$	$T_2^{(t)}$
−4	0.012	0.0112	−10	0.023	0.0236	−20	0.064	0.0628
−3	0.016	0.0150	−8	0.029	0.0296	−15	0.085	0.0838
−2	0.025	0.0224	−6	0.040	0.0394	−10	0.124	0.1256
–	–	–	−4	0.061	0.0592	−5	0.258	0.2514

coming back to the surface and the incident waves, then it is possible to derive a formula for the period of the oscillations using the basic dynamical theory of X-ray diffraction [in particular, using the property of the symmetrical Bragg case for crystals with a constant strain gradient that the tie point of the wave field going out of the crystals takes a position on the same branch of the dispersion surface that is symmetrical with respect to the reflecting planes (see Gronkowski & Malgrange, 1984)]. The simple formula found in this way for $\eta_r \gg 1$ is

$$T_2 = 2\pi B/|\eta_r|. \tag{24}$$

Table 4 shows the values calculated with formula (24) as compared with the values obtained from the full numerical calculations [Figs. 2(*a*), (*b*), (*c*)(i)]. It is readily seen that the approximate formula (24) works very well indeed for the values of $|\eta_r|$ not very close to 1. This is another proof that the oscillations originate from interferences between the incident and outgoing waves.

5.5. *Application of the oscillations for the XSW's*

The XSW signal on the oscillating flank is significantly influenced by the constant strain gradient in almost all cases studied. Except for cases of weak absorption and small gradients where the distances of the oscillation fringes are too small to be resolved in a real experiment, this feature may find a very interesting application, explained below:

Notice that the phase shift between the oscillations in the rocking curve and in the Y profile is directly related to $\Delta d/d$ [(17)]. The value of $\Delta d/d$ is easily determined if one takes into account that the phase shift in the particular case of $\Delta d/d = 0$ is equal to π for $B > 0$ and to 0 for $B < 0$ (Appendix B and Fig. 4). More generally, the phase shift expressed in units of 2π is equal to $\Delta d/d$ for $B < 0$ and $\Delta d/d + 0.5$ for $B < 0$.

6. Conclusions

We have used here a quasi-classical approximation to study the propagation of X-rays in cylindrically bent crystals. The range of validity of this approximation covers nearly all the values of incidence angles for small strain gradients (*e.g.* $4B = 0.001$) and decreases when the strain gradient increases (see Table 2). Within this approximation, it is shown that the shape of the rocking curve and of the XSW signal for a crystal with a constant strain gradient are practically the same as for a perfect one in the total reflection domain and on one flank of the rocking curve. On the other flank, however, there are oscillations that are shown to be due to interferences between the incident wave and the wave fields whose trajectories are curved back to the surface. They become negligible when absorption is large enough to attenuate the wave field in the crystal to a sufficiently low level; a quantitative criterion relating η_i, a parameter proportional to the ratio of the absorption coefficient to the structure factor of the given reflection, and the strain gradient $4B$ is given. For large absorption and small strain gradients, *i.e.* $\eta_i > 4B/3$, the oscillations disappear almost completely; if absorption is small ($\eta_i < 4B/3$), the rocking curve becomes enlarged due to the wave fields going out of the crystal surface. The values of the period of the fringes are calculated using the phase differences along the different curved trajectories.

It is shown by a simple argument developed in Appendix B that the oscillations of the rocking curve and of the standing-wave field at the reflecting planes ($\Delta d/d = 0$) are in phase or out of phase depending on the sign of B. Therefore, a simple measurement of

the phase shift between the oscillations on the rocking curve and, for example, on a fluorescence curve due to adatoms is a direct measure of the position of the adatoms with respect to the reflecting planes.

All these results have been derived from analytical results obtained for a constant strain gradient and an incident wave whose phase varies linearly on the entrance surface (*i.e.* cylindrically bent crystal and spherical wave with the source on the Rowland circle, or variation of lattice spacings and plane wave). They have been checked and illustrated for the simple symmetric case by computer experiments based on the Taupin equation; various values of the strain gradient and absorption were chosen so that η_i was either smaller or larger or equal to the critical value of $4B/3$.

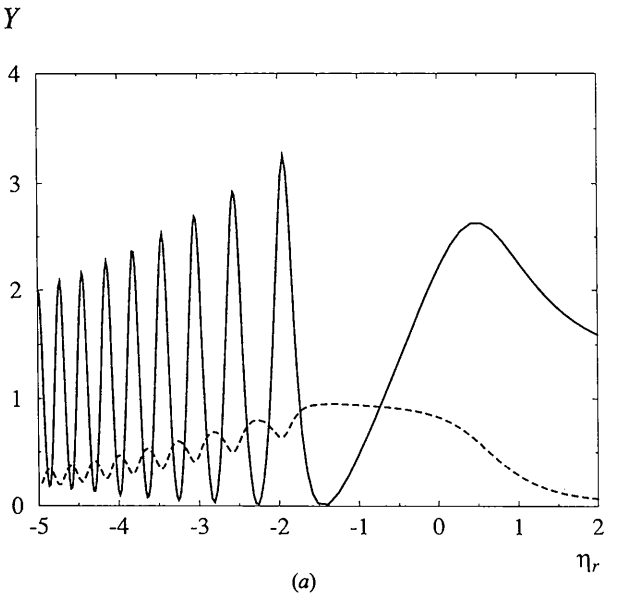

(*a*)

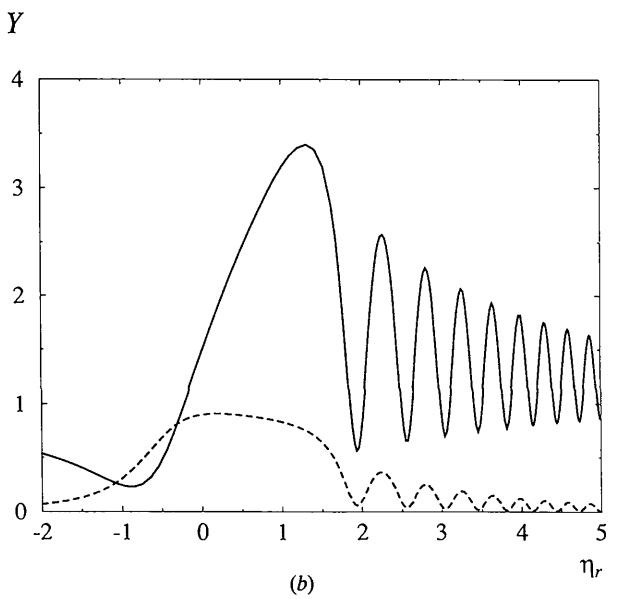

(*b*)

Fig. 4. The normalized wave-field intensity Y (full lines) and the rocking curves (dashed lines) as a function of the dimensionless deviation parameter η_r for: (*a*) $4B = 0.8$ and $\eta_r < -1$ [*cf.* Fig. 3(ii)(*c*)]; (*b*) $4B = -0.8$ and $\eta_r > 1$; GaAs 004 reflection, Cu $K\alpha_1$ radiation.

APPENDIX *A*
Quasi-classical approximation of parabolic cylinder function

We shall use, as in an earlier paper (Chukhovskii & Malgrange, 1989), the quasi-classical approximation of the parabolic cylinder functions valid for $|y^2+4\nu|^{1/2} \gg 1$:

$$\begin{aligned} D_{-n-\nu} = \exp[-\log(y^2+4\nu)/4] \\ \times \{C(n+\nu)\exp[-\theta_{n+\nu}(y)] \\ + \varepsilon[n+\nu,\chi]C^{-1}(n+\nu)(2\pi)^{1/2} \\ \times \Gamma^{-1}(n+\nu)\exp[\theta_{n+\nu}(y)]\}, \end{aligned} \tag{25}$$

where

$$\begin{aligned} \theta_{n+\nu}(y) &= y(y^2+4\nu)^{1/2}/4 + (n+\nu-\tfrac{1}{2}) \\ &\quad \times \log[y(y^2+4\nu)^{1/2}/2\nu^{1/2}], \end{aligned} \tag{26}$$

$$C(n+\nu) = \exp\{[\nu - (n+\nu-1/2)\log\nu]/2\}, \tag{27}$$

$$\varepsilon(n+\nu,\chi) = \begin{cases} 0 & \text{if } |\chi| \le \pi/4 \\ -\exp[-i\pi(n+\nu)] & \text{if } \pi/4 < \chi < 5\pi/4 \\ -\exp[i\pi(n+\nu)] & \text{if } -5\pi/4 < \chi < -\pi/4 \end{cases} \tag{28}$$

and χ is the phase of $(y^2+4\nu)^{1/2}$:

$$(y^2+4\nu)^{1/2} = |y^2+4\nu|^{1/2}\exp(i\chi). \tag{29}$$

Consequently, the second term of the development of $D_{-n-\nu}$ functions is zero if $|\chi| < \pi/4$. Therefore, let us discuss the phase χ of $(y^2+4\nu)^{1/2}$. If we write explicitly

$$y^2+4\nu = (i/B)[1-\eta_r^2+\eta_i^2-\kappa^2+2i(\kappa-\eta_r\eta_i)] \tag{30}$$

and define the phase angle ϕ of the term in the brackets as

$$\tan\phi = 2(\kappa-\eta_r\eta_i)/(1-\eta_r^2+\eta_i^2-\kappa^2) \tag{31}$$

such that $-\pi/2 < \phi < \pi/2$, then it is readily seen that the value of χ depends on the sign of $r = 1-\eta_r^2+\eta_i^2-\kappa^2$. Positive values of r correspond to the domain of 'total' reflection and $r < 0$ outside it. Besides, in most cases, $\eta_i^2 \ll 1$ and $\kappa^2 \ll 1$.

It can be shown that:

(i) if $r > 0$ (the domain of 'total' reflection), then $\chi = \text{sign}(B)(\pi/4) + \phi/2$ [where $\text{sign}(B) = 1$ for $B > 0$

and sign(B) $= -1$ for $B < 0$] and $|\chi| \leq \pi/2$, the two parabolic cylinder functions $D_{-\nu}$ and $D_{1-\nu}$ reduce to a single term;

(ii) if $r < 0$ (outside the domain of 'total' reflection), then $\chi = \text{sign}(B)(\pi/4) - \text{sign}(\eta_r)(\pi/2) + \phi/2$; several cases have to be distinguished depending on the signs of B and η_r (keeping in mind that $\phi > 0$ for $\eta_r > 1$ and $\phi < 0$ for $\eta_r < 1$):

(*a*) for $B > 0$ and $\eta_r > 1$, $\chi = -\pi/4 + \phi/2$; then $-\pi/4 < \chi < 0$;

(*b*) for $B < 0$ and $\eta_r < -1$, $\chi = \pi/4 + \phi/2$; then $0 < \chi < \pi/4$;

(*c*) for $B > 0$ and $\eta_r < -1$, $\chi = 3\pi/4 + \phi/2$; then $\pi/2 < \chi < 3\pi/4$;

(*d*) for $B < 0$ and $\eta_r > 1$, $\chi = -3\pi/4 + \phi/2$; then $-3\pi/4 < \chi < -\pi/2$.

In cases (*a*) and (*b*), $|\chi| < \pi/4$ and the functions $D_{-\nu}$ and $D_{1-\nu}$ reduce to a single term. Physically, these two cases correspond to ray paths curved towards the inside of the crystal [Fig. 1, trajectory (2)]. In cases (*c*) and (*d*) [Fig. 1, trajectory (1)], the second term in the asymptotic development is not zero.

Now we shall restrict ourselves to the cases where $D_{-\nu}$ and $D_{-1-\nu}$ reduce to the first terms. Strictly speaking, it means that we consider only values of η_r on the ordinary wing of the rocking curve. Then, from (25), (26) and (27), one readily obtains

$$\begin{aligned} D_{-1-\nu}(y)/D_{-\nu}(y) &= \{C(1-\nu)\exp[-\theta_{1+\nu}(y)]\}/\{C(-\nu)\exp[-\theta_\nu(y)]\} \\ &= 2/[y + (y^2 + 4\nu)^{1/2}], \end{aligned} \tag{32}$$

which can be substituted into (7).

APPENDIX *B*
The phase shifts of the oscillations in the XSW's and rocking curves

Let us denote the incident wave as D_o and the directly reflected wave as D_h. Then we have $D_h = \pm a D_o$, with $a > 0$ and the upper sign corresponding to $\eta_r > 1$, the lower one to $\eta_r < -1$ (as there is a phase shift between D_h and D_o equal to 0 and π in these two ranges, respectively). If we denote as $b\exp(i\varphi)D_o$ the diffracted wave issued from the curved wave field ($b > 0$), then the reflection coefficient R and the XSW yield Y will be given by

$$R = |\pm a + b\exp(i\varphi)|^2 = a^2 + b^2 \pm 2ab\cos\varphi, \tag{33}$$

$$\begin{aligned} Y(\Delta d/d = 0) &= |(1 \pm a) + b\exp(i\varphi)|^2 \\ &= (1 \pm a)^2 + b^2 + 2b(1 \pm a)\cos\varphi. \end{aligned} \tag{34}$$

R is maximum for $\varphi = \pi/2 + 2k\pi$ if $\eta_r > 1$ and $\varphi = -\pi/2 + 2k\pi$ if $\eta_r < -1$ while Y is maximum for $\varphi = \pi/2 + 2k\pi$ regardless of η_r. Therefore, if $\eta_r > 1$ and $B < 0$, the oscillations for R and Y are in phase; the reverse holds for $\eta_r < 1$ and $B > 0$.

References

Authier, A. & Balibar, F. (1970). *Acta Cryst.* A**26**, 647–654.

Authier, A., Gronkowski, J. & Malgrange, C. (1989). *Acta Cryst.* A**45**, 432–441.

Batterman, B. W. (1964). *Phys. Rev.* **133**A, 759–764.

Batterman, B. W. (1969). *Phys. Rev. Lett.* **22**, 703–705.

Chukhovskii, F. N., Gabrielyan, K. T. & Petrashen', P. V. (1978). *Acta Cryst.* A**34**, 610–621.

Chukhovskii, F. N. & Malgrange, C. (1989). *Acta Cryst.* A**45**, 732–738.

Gronkowski, J. (1991). *Phys. Rep.* **206**, 1–41.

Gronkowski, J. & Malgrange, C. (1984). *Acta Cryst.* A**40**, 507–514, 515–522.

Kato, N. (1964). *J. Phys. Soc. Jpn*, **19**, 67–77, 971–985.

Kjaer Andersen, S., Golovchenko, J. A. & Mair, G. (1976). *Phys. Rev. Lett.* **37**, 1141–1145.

Krisch, M. (1993). Thesis, University of Dortmund, Germany.

Malgrange, C. & Ferret, D. (1992). *Nucl. Instrum. Methods*, A**314**, 285–296.

Takagi, S. (1962). *Acta Cryst.* **15**, 1311–1312.

Takagi, S. (1969). *J. Phys. Soc. Jpn*, **26**, 1239–1253.

Taupin, D. (1964). *Bull. Soc. Fr. Minéral. Cristallogr.* **87**, 469–511.

Uschmann, I., Förster, E., Gäbel, K., Hölzer, G. & Ensslen, M. (1993). *J. Appl. Cryst.* **26**, 405–412.

Vartanyantz, I. A., Kovalchuk, M. V. & Beresovsky, V. M. (1993). *J. Phys. D*, **26**, A197–A201.

Zegenhagen, J. (1993). *Surf. Sci. Rep.* **18**, 199–271.